Publication P5

Sami Ruoho, Minna Haavisto, Eelis Takala, Timo Santa-Nokki, and Martti Paju. 2010. Temperature dependence of resistivity of sintered rare-earth permanent-magnet materials. IEEE Transactions on Magnetics, volume 46, number 1, pages 15-20.

Temperature Dependence of Resistivity of Sintered Rare-Earth Permanent-Magnet Materials

Sami Ruoho[1,2], Minna Haavisto[3], Eelis Takala[3], Timo Santa-Nokki[3], and Martti Paju[3]

[1]Laboratory of Electromechanics, Helsinki University of Technology, FIN-02015 TKK, Finland
[2]Neorem Magnets Oy, FIN-28400 Ulvila, Finland
[3]Magnet Technology Centre, Prizztech Oy, Teknologiakeskus Pripoli FIN-28600 Pori, Finland

We studied the resistivity of rare-earth permanent-magnet materials over the temperature range $-40°C$ to $+150°C$. We investigated three different materials from four manufacturers, including $Nd_2Fe_{14}B$, $SmCo_5$, and Sm_2Co_{17}, and measured their resistivities and temperature coefficients. We found that rare-earth permanent-magnet materials show an anisotropic resistivity behavior. In fact, the resistivity anisotropy causes larger resistivity difference than the temperature variation within the range studied. In many applications, such as permanent-magnet motors, this behavior has to be taken into account in design.

Index Terms—**Conductivity, permanent magnet, rare-earth, resistivity.**

I. Introduction

THE exact knowledge of the permanent-magnet material resistivity is important when modeling applications, where eddy currents can be present. For instance, in the design of permanent-magnet motors, which can work over a very wide temperature range, the temperature dependence of resistivity of permanent-magnet material is needed to allow an accurate eddy-current modeling.

Typically, the resistivity is assumed to be isotropic and constant over the temperature range occurring in the application. Thus, only single values are commonly given to permanent-magnet material resistivities or conductivities in standard [1] or in the brochures of the manufacturers [2]. In previous publications concerning eddy-current calculations, the authors have used the room-temperature resistivity values according to the IEC standard [6]–[8]. Temperature dependency or anisotropy is not mentioned.

There are very few publications about the temperature dependency of the electrical resistivity of rare-earth permanent-magnet materials. Some resistivity measurements for Nd-Fe-B alloys are reported [3]–[5]. However, temperature dependence data for resistivity of commercially available rare-earth permanent magnets cannot be found in the literature.

In [9], the resistivity of anisotropic permanent-magnet materials is mentioned to be anisotropic. However, values of resistivity or the difference of the resistivity in different directions are not given.

II. Research Interests

There were four different interests in this research. These are discussed in the following subchapters.

Manuscript received June 19, 2008; revised December 23, 2008. Current version published December 23, 2009. Corresponding author: S. Ruoho (e-mail: sami.ruoho@neorem.fi).

Digital Object Identifier 10.1109/TMAG.2009.2027815

A. The Temperature Dependence of Resistivity

The main purpose of this research was to measure the temperature dependence of resistivity of three different rare-earth permanent-magnet materials. The studied temperature range was $-40°C$ to $+150°C$, which covers the normal working conditions of many permanent-magnet applications.

B. Effect of Orientation Direction on Resistivity

Since the magnetic properties of the rare-earth permanent-magnet materials are anisotropic, the anisotropy of the resistivity also needs to be studied.

C. Effect of Magnetization on Resistivity

The effect of magnetization on resistivity was also studied. Comparison was made between nonmagnetized and magnetized samples. This comparison was made only at room temperature.

D. Effect of Dy Content of Nd-Fe-B Magnet on Resistivity

There are several different Nd-FeB magnet grades with different magnetic properties. High remanence magnets contain only small amount of dysprosium (Dy). By increasing the Dy content, higher intrinsic coercivities can be achieved. Simultaneously, the remanence will decrease. Thus, by varying the chemical composition of Nd-Fe-B magnets, different magnetic properties can be achieved.

The effect of the chemical composition of different Nd-Fe-B grades on resistivity was the fourth interest of this study.

III. Samples

In this research, three different sintered permanent-magnet materials were used: $SmCo_5$, Sm_2Co_{17}, and $Nd_2Fe_{14}B$. Commercial magnets of Chinese and European origin were selected for the study. The different manufacturers are referred as manufacturers A, B, C, and D in this paper.

All samples had cylindrical shape with length of 20 mm and diameter of 4 mm. Both magnets with orientation to axial direction (magnetization along the cylinder axis) and to transversal direction (magnetization perpendicular to cylinder axis) were prepared from all the materials.

The chemical composition of tested $SmCo_5$ and Sm_2Co_{17} samples and Nd-Fe-B samples from manufacturer C is not known. According to the manufacturer A, the $SmCo_5$ and $Sm_2[Co, Fe, Cu, Zr]_{17}$ samples tested represent the typical compositions of these materials.

The Nd-Fe-B samples from manufacturer D have a total rare-earth content of 31% to 32.5%. Dy content of Nd-Fe-B samples varied between 1% and 9%. In the sample, which had 1% Dy, also praseodymium (Pr) was present. Other rare-earth metals were not used. The samples from manufacturer D were cobalt-free.

IV. Measurement Setup

The resistivity measurements were performed accordingly: The voltage loss V along a known distance l over the sample was measured when constant current I was flowing through the sample. The resistivity ρ can be calculated according to (1). Measured values for sample diameter D were used

$$\rho = \frac{V\pi\left(\frac{D}{2}\right)^2}{Il}. \tag{1}$$

The measurement setup was specially designed for four point contact resistivity measurements for D4 × 20 cylindrical shaped samples. Special jigs were built to hold the samples. KEPCO BOP 20-20 M current source was used to generate and to measure the test current through the sample. Agilent 34410a-multimeter was used to measure the voltage drop in the sample. The devices were controlled by a program written on LabView.

The measurements were performed over the temperature range $-40°C$ to $+150°C$. The actual measurement temperatures were $-40°C$, $-20°C$, $0°C$, $+24°C$, $+60°C$, $+80°C$, $+120°C$, and $+150°C$. Elevated temperatures were generated by StabiliTherm EU2 ovens. Temperatures were measured with a calibrated thermocouple.

The final resistivity result is an average of three individually calculated resistivity values at each temperature. Measurements for these resistivity calculations were made in 30–60 s periods. Each measurement consists of ten voltage drop measurements within one second. The average of these voltage losses is used in resistivity calculation.

V. Error Sources

In this chapter, the possible error sources in the measurements are discussed.

A. Accuracy of Temperature

The measurement temperatures were achieved by different means, and thus the accuracy of temperatures varies. Estimated accuracies of different temperatures are described in Table I.

B. Sample Heating Caused by the Current

The measurement current I flows through the sample along its length l of 20 mm causing Joule heating. The rate of temperature rise is

$$\frac{\Delta T}{\Delta t} = \frac{\rho I^2}{A^2 \rho_m c} \tag{2}$$

where

ΔT is the temperature rise (°C);
Δt is the duration of the measurement (s);
ρ is the specific electrical resistivity of the sample (Ωm);
I is the measuring current (A);
A is the area of the sample (m^2);
ρ_m is the density of the sample (kg m^{-3}) and c is the specific heat of the sample material (J kg^{-1} K^{-1}).

The length of the sample does not have an effect on the sample heating rate, as can be seen from (2).

The measurement current in each case was 1 A. The rate of the temperature rise in each sample material due to measurement current is presented in Table II.

The duration of each measurement was approximately 1 s, which corresponds to a temperature rise of less than 3 mK. This temperature rise is a lot smaller than the accuracy of the temperature measurement, and can thus be ignored.

C. Distribution of the Measurement Current

The distribution of the voltage on the surface of a sample is presented in Fig. 1. The plot is based on finite element method calculations in which the resistivity of the magnet was 1.5 μΩm and the measurement current through the sample 1 A. The diameters of supply conductors and the sample were 0.4 mm and 4 mm, respectively, and the length of the sample was 20 mm as in the resistivity measurements.

The linear region, which is suitable for the measurement of voltage loss, is approximately 16 mm wide, and it could be extended by enlarging the cross-sectional area of the supply conductors. The distance between measurement points was set to 10 mm to be safely on the linear area.

TABLE I
Accuracy of Different Temperatures

Measurement Temperature	Accuracy of the Measurement Temperature
-40°C	±0.5°C
-20°C	±2°C
0°C	±2°C
+24°C	±0.5°C
+60°C	±0.5°C
+80°C	±0.5°C
+120°C	±0.5°C
+150°C	±1°C

TABLE II
Heating Rates of Different Sample Materials During Measurements

Material	ρ ($\Omega mm^2 m^{-1}$)	c (J $kg^{-1}K^{-1}$)	ρ_m (kg m^{-3})	$\Delta T/\Delta t$ (K s^{-1})
NdFeB	1.5	450	7600	0.0028
$SmCo_5$	0.55	400	8400	0.0010
Sm_2Co_{17}	0.7	400	8400	0.0013

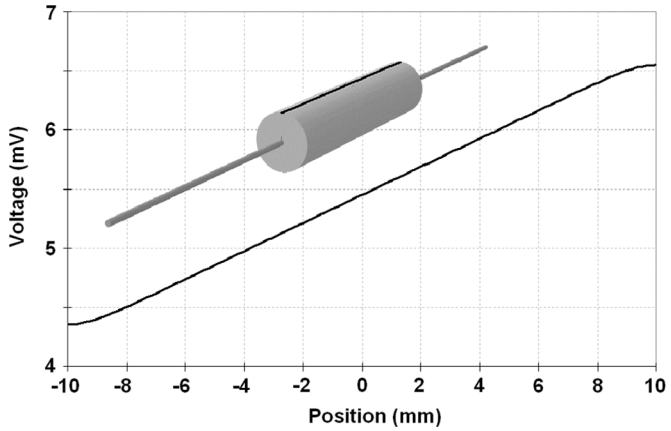

Fig. 1. Voltage profile on the surface of the resistivity sample in the four-point measurement. The voltage drop was measured from the linear part of the curve. The distance between the measurement probes from the sample ends was 5 mm. Sample length was 20 mm and diameter 4 mm.

TABLE III
TEST PARAMETERS

Quantity	Symbol	Value	Accuracy
Current	I	1 A	20 mA
Voltage	V	Not constant	3.5 μV
Radius	r	2 mm	0.02 mm
Measuring length	l	10	0.02 mm

D. Measurement Accuracy

By using the intermediate value theorem on (1), the absolute maximum error can be written

$$\Delta\rho \leq \left(\left| \frac{2\Delta r}{r} \right| + \left| \frac{\Delta I}{I} \right| + \left| \frac{\Delta l}{l} \right| \right) \rho + \left| \frac{\pi r^2 \Delta V}{Il} \right| \quad (3)$$

where r is the radius of the cylinder (m).

The accuracy specifications for Agilent 34410a in "dc-voltage"-mode are 0.004% of reading and 0.0035% of range (100 mV). The reading error is very small compared to the range error due to small readings (few millivolts) and can thereby be neglected. Thus, ΔV is 3.5 μV.

The accuracy specification for KEPCO BOP 20-20 M current source is 20 mA for measurement accuracy.

The test parameters are listed in Table III. Now, (3) yields

$$\Delta\rho \leq 0.042\rho + 4.40\text{n}\Omega\text{m}. \quad (4)$$

The absolute error, when the value of ρ varies between 0.3 $\mu\Omega$m and 1.6 $\mu\Omega$m (according to [1]), is expected to be around 5% according to (4).

VI. RESULTS

A. SmCo-Samples

Resistivities of different SmCo-samples at 24°C are compared in Fig. 2. Results for temperature dependence of resistivity of $SmCo_5$ samples can be found in Fig. 3. Results for temperature dependence of resistivity of Sm_2Co_{17} samples can be found in Fig. 4.

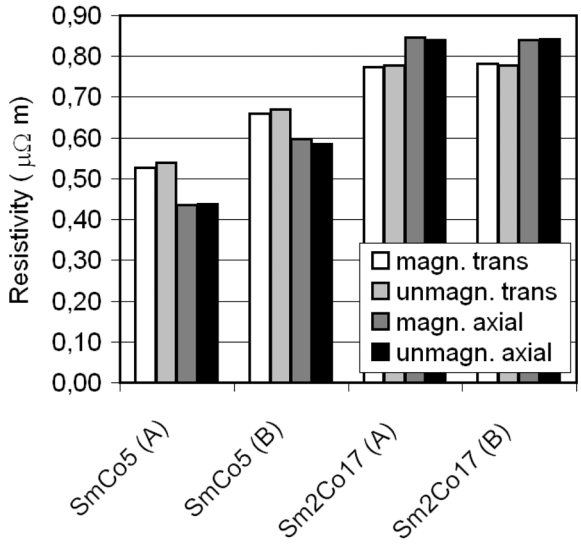

Fig. 2. Resistivities of SmCo-samples at 24°C. The resistivity is presented both in axial and in transversal direction relative to the axis of orientation. Both magnetized and unmagnetized samples from two manufacturers (A and B) were used.

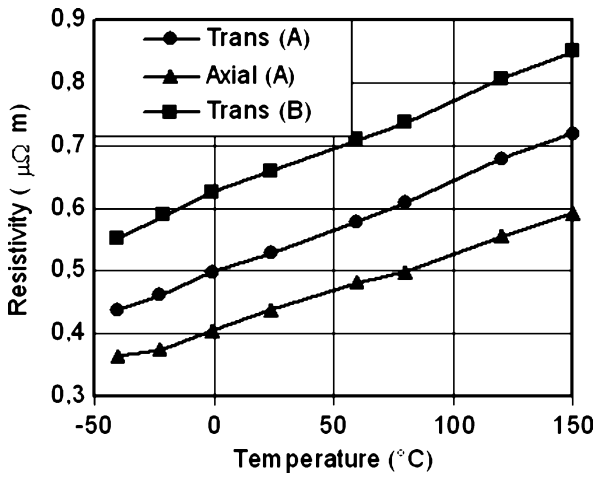

Fig. 3. Resistivity of magnetized $SmCo_5$ samples from manufacturers A and B as a function of temperature. The resistivity is presented both in axial and in transversal direction relative to the axis of orientation.

B. Nd-Fe-B Samples

Average resistivities of different Nd-Fe-B samples at 24°C are compared in Fig. 5. Resistivity as a function of Dy content can be found in Fig. 6. Results for temperature dependence of resistivity of Nd-Fe-B samples can be found in Fig. 7.

C. Curve Fitting

Curves were fitted to measurement data to allow easy calculation of resistivity at different temperatures. First-order polynomials modeled the temperature behavior of the most measured

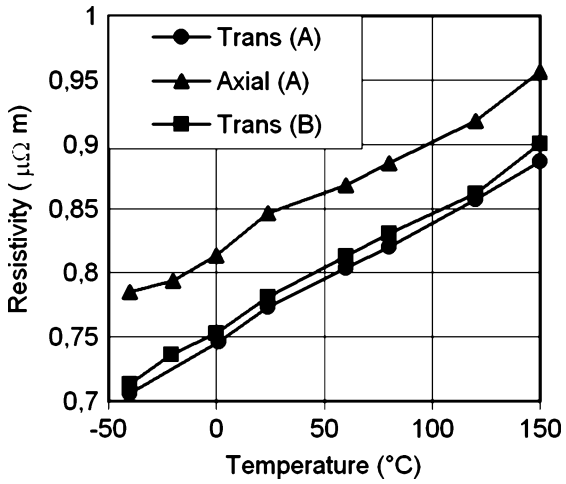

Fig. 4. Resistivity of magnetized Sm_2Co_{17} samples from manufacturers A and B as a function of temperature. The resistivity is presented both in axial and in transversal direction relative to the axis of orientation.

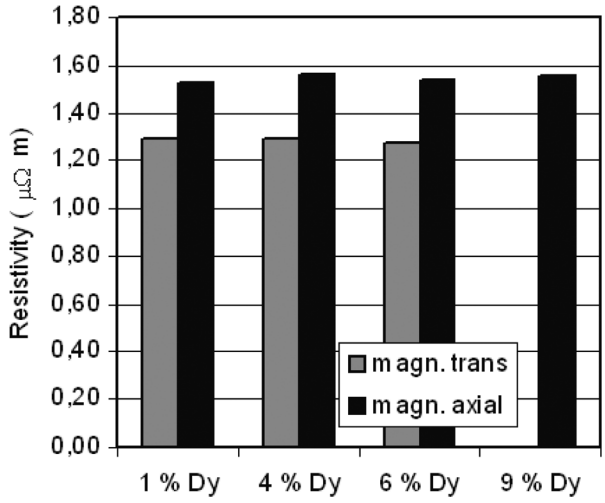

Fig. 6. Resistivities of magnetized Nd-Fe-B-samples with different Dy content from manufacturer D at 24°C. The resistivity is presented both in axial and in transversal direction relative to the axis of orientation.

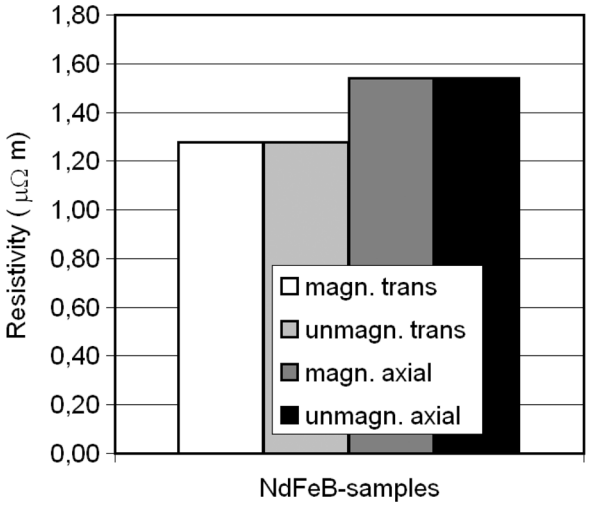

Fig. 5. Average resistivities of Nd-Fe-B-samples at 24°C. The resistivity is presented both in axial and in transversal direction relative to the axis of orientation. Five axial and four transversal samples were measured. Both magnetized and unmagnetized samples were used.

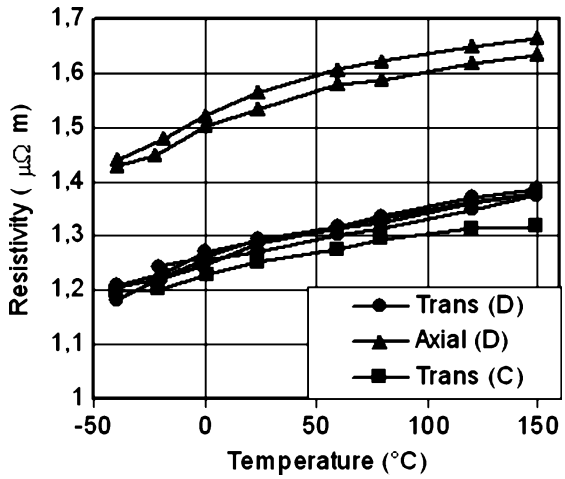

Fig. 7. Resistivity of magnetized Nd-Fe-B-samples from manufacturers C and D as a function of temperature. The resistivity is presented both in axial and in transversal direction relative to the axis of orientation.

samples well and, thus, curves according to (5) were fitted

$$\rho(\mu\Omega\mathrm{m}) = \mathrm{b}\cdot\mathrm{T}(^{\circ}\mathrm{C}) + \mathrm{a}. \tag{5}$$

The measurements of axially oriented Nd-Fe-B samples showed nonlinear behavior, which could be modeled quite accurately with a second-order polynomial

$$\rho(\mu\Omega\mathrm{m}) = \mathrm{c}\cdot(\mathrm{T}(^{\circ}\mathrm{C}))^2 + \mathrm{b}\cdot\mathrm{T}(^{\circ}\mathrm{C}) + \mathrm{a}. \tag{6}$$

The curve fitting results are presented for $SmCo_5$ and Sm_2Co_{17} samples in Tables IV and V, respectively. The curve fitting results for the transversal resistivity of Nd-Fe-B magnets can be found in Table VI. The curve fitting results for the axial resistivity of Nd-Fe-B magnets can be found in Table VII.

TABLE IV
RESISTIVITIES AND CURVE FITTING DATA FOR MAGNETIZED $SmCo_5$ MATERIAL SAMPLES

Manufacturer	Orientation of sample	Measured resistivity at 24°C (μΩ m)	b in (5) $\cdot 10^{-3}$	a in (5)	Calculated resistivity according to (5) at 20°C (μΩ m)
A	Transversal	0.53	1.48	0.495	0.52
A	Axial	0.44	1.23	0.406	0.43
B	Transversal	0.66	1.54	0.619	0.65
B	Axial	0.60	-	-	-

VII. DISCUSSION

A. Effect of Magnetization on Resistivity

Comparison of the resistivities of Nd-Fe-B samples at room temperature (see Fig. 5) revealed that the average difference between magnetized and unmagnetized samples is only 0.1%. The same difference for $SmCo_5$ samples is 0.5% and for Sm_2Co_{17}

TABLE V
RESISTIVITIES AND CURVE FITTING DATA FOR MAGNETIZED Sm_2Co_{17} MATERIAL SAMPLES

Manufacturer	Orientation of sample	Measured resistivity at 24°C (μΩ m)	b in (5) $\cdot 10^{-3}$	a in (5)	Calculated resistivity according to (5) at 20°C (μΩ m)
A	Transversal	0.77	0.939	0.746	0.76
A	Axial	0.85	0.893	0.817	0.83
B	Transversal	0.78	0.948	0.754	0.77
B	Axial	0.84	-	-	-

TABLE VI
RESISTIVITIES AND CURVE FITTING DATA FOR TRANSVERSAL RESISTIVITY OF MAGNETIZED Nd-Fe-B MATERIAL SAMPLES

Dy-content	Orientation of sample	Measured resistivity at 24°C (μΩ m)	b in (5) $\cdot 10^{-3}$	a in (5)	Calculated resistivity according to (5) at 20°C (μΩ m)
1 %	Transversal	1.29	0.933	1.248	1.27
4 %	Transversal	1.29	0.884	1.258	1.28
6 %	Transversal	1.27	0.936	1.240	1.26
N.A.	Transversal	1.25	0.699	1.227	1.24

TABLE VII
RESISTIVITIES AND CURVE FITTING DATA FOR AXIAL RESISTIVITY OF MAGNETIZED Nd-Fe-B MATERIAL SAMPLES

Dy-content	Measured resistivity at 24°C (μΩ m)	c in (6) $\cdot 10^{-6}$	b in (6) $\cdot 10^{-3}$	a in (6)	Calculated resistivity according to (6) at 20°C (μΩ m)
4 %	1.57	-5.468	1.765	1.520	1.53
6 %	1.53	- 4.580	1.591	1.496	1.55

magnets 0.1% (see Fig. 2). These differences are within the measurement errors. It can be concluded that the magnetization does not have a significant effect on the resistivity of the material.

B. Effect of Orientation Direction on Resistivity

Figs. 2 and 5 show clearly that the resistivity of the rare-earth permanent-magnet materials show anisotropic behavior. The average difference between transversally and axially oriented Nd-Fe-B-samples is approximately 18%. This can be qualitatively understood, as the crystal structure and magnetic properties of these materials are also anisotropic.

The resistivity in the magnetic orientation direction (or in the axial direction) was larger than the resistivity in the transversal direction (or in the direction perpendicular to the orientation direction) in Nd-Fe-B samples and in Sm_2Co_{17} samples. $SmCo_5$ samples showed opposite behavior: the transversal resistivity was larger than the axial.

The anisotropic behavior of resistivity is important to notice. The difference in resistivity caused by the anisotropy is larger than the one caused by the temperature change in many application, like permanent-magnet electric machines. Thus, in accurate eddy-current calculations, the anisotropy of resistivity of the rare-earth permanent magnets should be taken into account.

TABLE VIII
IEC STANDARD VALUES AND MEASURED VALUES FOR RESISTIVITIES

Material (Manufacturer)	IEC Standard value for resistivity (μΩ m) [1]	Measured resistivity in transversal direction at 24°C (μΩ m)	Measured resistivity in axial direction at 24°C (μΩ m)
Nd-Fe-B (C & D)	1.4…1.6	1.25…1.29	1.51…1.57
$SmCo_5$ (A)	0.5…0.6	0.53	0.44
$SmCo_5$ (B)		(0.66)	(0.60)
Sm_2Co_{17} (A & B)	0.75…0.85	0.77…0.78	0.84…0.85

C. Effect of Temperature on Resistivity

The temperature dependence of resistivity of the rare-earth magnet materials is linear at the temperature range of this study. The only exception is the axial resistivity of Nd-Fe-B material, which showed nonlinear behavior, as can be seen in Fig. 7.

D. Effect of Dy Content of Nd-Fe-B Magnet on Resistivity

The varying Dy content in Nd-Fe-B samples did not cause difference in resistivity, as can be seen in Fig. 6.

E. SmCo-Samples

Sm_2Co_{17} samples from manufacturers A and B showed similar resistivity. However, the properties of the $SmCo_5$ sample from the manufacturer B was somewhere between the properties of Sm_2Co_{17} samples and $SmCo_5$ sample from manufacturer A.

F. Resistivity Values in IEC Standard

Measured resistivities at room temperature and the resistivities found in IEC standard [1] are compared in Table VIII. It can be noticed that these values for Nd-Fe-B material resistivity correspond to the resistivity in axial direction. The measured resistivity of Nd-Fe-B samples in the transversal direction is approximately 18% lower than the resistivity in the axial direction. The resistivity in the transversal direction does not fall into the range presented in the standard.

The measured transversal resistivity of the $SmCo_5$ sample from manufacturer A falls into the range presented in the standard, but the measured axial resistivity is below the lower limit. The transversal resistivity of the $SmCo_5$ sample from manufacturer B is clearly above the upper limit presented in the standard and also the axial resistivity is on the upper limit.

The anisotropy of resistivity of Sm_2Co_{17} material is smaller, and both axial and transversal measured resistivities fall into the range presented in the standard.

VIII. CONCLUSION

The temperature dependence of resistivity of Nd-Fe-B, $SmCo_5$, and Sm_2Co_{17} rare-earth permanent-magnet materials was studied, as well as the effects of magnetization, orientation, and chemical composition on the resistivity. Magnetization or variation in chemical composition was not observed to have an effect on the resistivity.

Orientation was found to have a significant effect on the resistivity. Resistivity needs to be considered as anisotropic characteristic in the rare-earth permanent-magnet materials. This leads to the conclusion that in accurate eddy-current calculations, 3-D anisotropic models are required.

The temperature dependence of resistivity of the rare-earth materials was found to be linear within the studied temperature range $-40°$C to $+150°$C. Only the resistivity of Nd-Fe-B magnet in axial direction (in the orientation direction) showed significantly nonlinear behavior.

ACKNOWLEDGMENT

This work was supported by Finnish Cultural Foundation, Research Foundation of Helsinki University of Technology, Ulla Tuomisen Säätiö, High Technology Foundation of Satakunta, and European Regional Development Fund.

REFERENCES

[1] *Specifications for Individual Materials—Magnetically Hard Materials*, IEC standard: 60404-8-1, 2004, p. 65, IEC:2001+A1.

[2] *PD 002-VACODYM/VACOMAX·EDITION 2007 S. The Brochyre Permanent Magnets*, [Online]. Available: http://www.vacuumschmelze.de/dynamic/docroot/medialib/documents/broschueren/dm-brosch/PD-002_e_310807.pdf, pp. 14–17, 07.02.2008

[3] S. U. Jen and Y. D. Yao, "Electrical resistivity and specific heat studies of Nd-Fe-B magnet around its $\mathrm{T_C}$," *J. Appl. Phys.*, vol. 61, no. 8, pp. 4252–4254, 1987.

[4] Y. D. Yao, "Electrical resistivity and magnetization studies of the NdFeB system," *Chin. J. Phys.*, vol. 26, no. 4, 1988.

[5] K. T. Wu and Y. D. Yao, "Electrical and magnetic properties of NdFeB films," *Appl. Surf. Sci.*, pp. 174–177, 1997, 113-114:.

[6] D. Ishak, Z. Zhu, and D. Howe, "Eddy-current loss in the rotor magnets of permanent-magnet brushless machines having a fractional number of slots per pole," *IEEE Trans. Magn.*, vol. 41, no. 9, pp. 2462–2469, Sep. 2005.

[7] M. Markovic and Y. Perriard, "Analytical solution for rotor eddy-current losses in a slotless permanent-magnet motor: The case of current sheet excitation," *IEEE Trans. Magn.*, vol. 44, no. 3, pp. 386–393, Mar. 2008.

[8] J. Ede, K. Atallah, and D. Howe, "Effect of axial segmentation of permanent magnets on rotor loss in modular permanent-magnet brushless machines," *IEEE Trans. Ind. Appl.*, vol. 43, no. 5, pp. 1207–1213, Sep./Oct. 2007.

[9] O. Gutfleisch, M. Verdier, I. Harris, and A. Ray, "Characterisation of rare earth-transition metal alloys with resistivity measurements," *IEEE Trans. Magn.*, vol. 29, no. 6, pp. 2872–2874, Nov. 1993.